International Journal of Railway Research, Vol. 7, No. 2, (2020), 35-43

Iran University of Science and Technology

International Journal of

Railway Research

Three-Port Multifunctional Railway Power Conditioner Integrated with Energy Storage Systems for Regenerative Braking Energy and Power Quality Control

Hamed Jafari Kaleybar[1*], Seyed Saeed Fazel[2]

[1]Energy Department, Politecnico di Milano, Milan, Italy

[2]School of Railway Engineering, Iran University of Science and Technology, Tehran, Iran

ARTICLE INFO

Article history:
Received: 11.05.2020
Accepted: 27.07.2020
Published: 25.12.2020

Keywords:
Electric railway
Energy storage system
Regenerative braking energy
Power quality
Power flow control

A B S T R A C T

Electrical railway systems (ERSs) are one of the largest end-users in the utility grid. Providing optimal energy management and improving efficiency in such a high-power network is a vital approach to conserve energy and decrease economic costs. Meanwhile, proper exploitation of regenerative braking energy (RBE) as a dormant potential in ERSs, is a distinguished opportunity to achieve these goals. This paper presents a proposal to achieve the mutual advantages of RBE harvesting and energy storage systems (ESSs). In the proposed strategy, a multifunctional railway power conditioner (MF-RPC) together with its smart control system is employed to realize the optimal mode of the active and reactive powers exchange in output ports. Depending on the motoring and generating powers of trains on both sides of traction substation (TSS), the proposed MF-RPC can simultaneously restore back RBE to the grid, save energy in ESSs and power other adjacent consuming trains. Regarding the intrinsic features of MF-RPC, all proposed scenarios are consistent with power quality standards. The simulation results based on MATLAB/SIMULINK are provided to confirm the effectiveness of the proposed method.

1. Introduction

Nowadays, different transportations systems are striving to have higher energy efficiency and better environmental performance together with a significant reduction in costs. Among these, electrical railway systems due to some advantages like high safety, low cost of operation and high capacity are considered as the foremost economical and sustainable means of transport [1-3]. However, with the rapid developments of smart grid concepts in various industrial sectors, to maintain ERS inherent privileges in terms of energy consumption, important energy management strategies have to be implemented. Regenerative braking energy as a dormant potential in ERSs is considered an appropriate approach and a key role in increasing energy efficiency. During last years, many studies are dedicated to present different RBE harvesting procedures consisting timetable optimization [4], saving energy to onboard and wayside ESSs [5, 6], supplying another adjacent train in the same section [7], and restoring back the energy to the distribution grid in a reversible substations [8, 9]. Due to the multiple stops and a short distance of stations, the majority of these studies have been concentrated on urban rail transport such as tramway, light rail transport, monorail, and metro (DC traction systems) [10-14]. However, given that the amount generated RBE is proportional to the train mass, the pattern of deceleration and the square of velocity, the potential of RBE utilization in AC and high-speed railway lines are so remarkable to be considered due to the high-power and high-speed trains. On the other side, the inherent

*Corresponding author, Research fellow
Email: hamed.jafari@polimi.it

[DOI: 10.22068/IJRARE.7.2.35]

features of AC ERSs with fundamental power quality (PQ) problems make it arduous to exploit RBE.

Consequently, most of the railway companies are reluctant to utilize extracted RBE because it may not comply with the related PQ standards. Meanwhile, the national utility grid desires for acceptable compliance with the PQ standards to allow RBE restoring to the grid. As a result, implementing these commitments on both sides of the energy cycle increases to the challenges of RBE exploitation. Despite the difficulties, there are some researches that have addressed to utilize the RBE in AC ERSs. A model for direct restoring of RBE to the AC grid is presented in [15], which contains limitations in compensating voltage fluctuation and other PQ problems. Some methods based on timetable optimization and optimal driving, are presented in [16] but these procedures are not assumed possible PQ issues. In [17] a storage system based on high power lithium cells is proposed to recover RBE. This method has not addressed restoring RBE to the utility grid. In addition, this system is presented for DC ERSs. In [18], the potential of harvesting RBE in AC and high-speed ERSs are studied. The field measurements of this paper reveal that the total reversed RBE in 17 traction substations can exceed 200MWh/day. However, more than 50% of this energy can't be exploited because at the moment of RBE generation there is no train in the same section. Furthermore, this method is not capable of restoring energy to the utility grid. Motivated by the above descriptions, this paper proposes a multifunctional railway power conditioner (MF-RPC) which acts as an energy hub performing an optimal power flow and energy transfer in TSS. A smart multi-loop generalized control method is proposed to manage all possible scenarios related to power transferring in TSS compliant with PQ standards.

2. Proposed MF-RPC Principles

The structure of proposed MF-RPC in a TSS of 1×25 kV supply system is shown in Fig.1. The MF-RPC is composed of two back-to-back converters with a shared DC-link capacitor and two single-phase step-down transformers connected to both sides of TSS named as α and β sections. The third port of proposed MF-RPC is connected to the ESSs through a DC link.

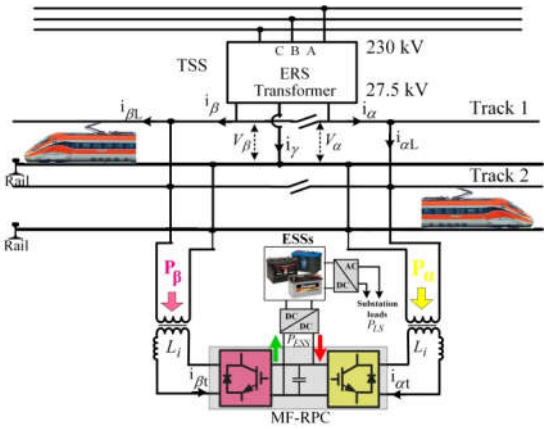

Figure 1. Configuration of TSS with proposed MF-RPC integrated with ESSs

To attain the reference voltages and currents with Yd power transformer in TSS, the load imbalance coefficients are described as the ratio of locomotive actual currents to the full load current of the locomotive in sections. Meanwhile, ζ_α and ζ_β are determined as the load imbalance ratio (LIR) of α and β sections respectively. The phase and line voltages in primary-side (PrS) and secondary-side (SrS) of TSS are assumed as (1) and (2).

$$\begin{cases} V_A(t) = \mathbf{Re}\left\{\mathbf{V}_A e^{i(\omega t)}\right\} = \mathbf{Re}\left\{V e^{i(\omega t+\theta_a)}\right\} \\ V_B(t) = \mathbf{Re}\left\{\mathbf{V}_B e^{i(\omega t)}\right\} = \mathbf{Re}\left\{V e^{i(\omega t+\theta_a+\frac{4\pi}{3})}\right\} \\ V_C(t) = \mathbf{Re}\left\{\mathbf{V}_C e^{i(\omega t)}\right\} = \mathbf{Re}\left\{V e^{i(\omega t+\theta_a+\frac{2\pi}{3})}\right\} \end{cases} \quad (1)$$

$$\begin{cases} V_\alpha(t) = V_{ac}(t) = \dfrac{\sqrt{3}}{K_a}\mathbf{Re}\left\{V e^{i(\omega t+\psi)}\right\} \\ V_\beta(t) = V_{bc}(t) = \dfrac{\sqrt{3}}{K_a}\mathbf{Re}\left\{V e^{i(\omega t+\psi-\frac{\pi}{3})}\right\} \end{cases} \quad (2)$$

Where V is the rms value of phase voltage, ψ is the phase angle of $\dot{V}_\alpha$ and K_a is the turn ratio of the transformer. To have inductance property of trains in equations, it is assumed that the section currents lag the voltages by φ_a, φ_b. According to the selected Yd transformer vector group, the PrS currents can be calculated as (3). The phasor diagram related to the TSS voltages and currents is shown in Fig. 2. It is obvious that the current in the two sections is imbalanced and the PrS currents are asymmetrical. To balance the currents, the difference of the consumed currents in α and β sections should be

[DOI: 10.22068/IJRARE.7.2.35]

transferred from the light section to the high one as (4) [19]. This will attain to the currents relations of (5) for each section.

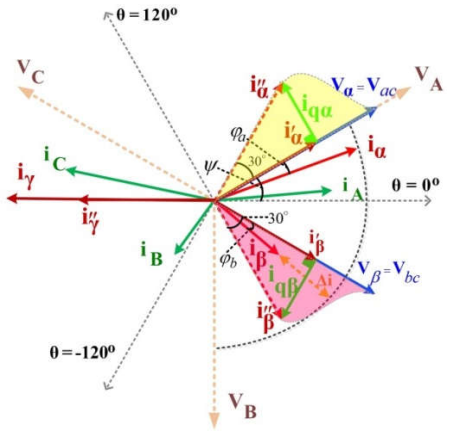

Figure 2. Voltage and current phasor diagram of proposed TSS integrated with MF-RPC

$$\begin{cases} i_a = i_\alpha = \zeta_\alpha I \ \mathbf{Re}\left\{e^{i(\omega t+\psi-\varphi_a)}\right\} \\ i_b = i_\beta = \zeta_\beta I \ \mathbf{Re}\left\{e^{i(\omega t+\psi-\frac{\pi}{3}-\varphi_b)}\right\} \\ i_c = i_\gamma = -(i_\alpha + i_\beta) = -I \begin{pmatrix} \zeta_\alpha \mathbf{Re}\left\{e^{i(\omega t+\psi-\varphi_a)}\right\} \\ +\zeta_\beta \mathbf{Re}\left\{e^{i(\omega t+\psi-\frac{\pi}{3}-\varphi_b)}\right\} \end{pmatrix} \end{cases} \quad (3)$$

$$\Delta i = |\mathbf{i}_\alpha| - |\mathbf{i}_\beta| = I|\zeta_\alpha - \zeta_\beta| \quad (4)$$

$$\mathbf{i}'_\alpha = (|\mathbf{i}_\alpha| - \frac{\Delta i}{2})e^{i\psi} \ , \mathbf{i}'_\beta = (|\mathbf{i}_\beta| + \frac{\Delta i}{2})e^{i(\psi-\frac{\pi}{3})} \quad (5)$$

Due to the lead and lagged property of sections, by transmitting these currents the PrS currents will not be symmetrical. To make the currents balanced completely, the reactive component currents ($i_{q\alpha}, i_{q\beta}$) must be added to each section as follows:

$$\mathbf{i}_{q\alpha} = tg30^\circ \times \mathbf{i}'_\alpha e^{i\frac{\pi}{2}}, \ \mathbf{i}_{q\beta} = tg30^\circ \times \mathbf{i}'_\beta e^{-i\frac{\pi}{2}} \quad (6)$$

The reactive component currents are absorbed in the lead section and transferred to the lagging section by MF-RPC as in Fig. 2. Finally, the PrS currents can be derived as:

$$\begin{cases} \mathbf{i}''_\alpha = \mathbf{i}'_\alpha + \mathbf{i}_{q\alpha} \\ \mathbf{i}''_\beta = \mathbf{i}'_\beta + \mathbf{i}_{q\beta} \\ \mathbf{i}''_\gamma = -(\mathbf{i}''_\alpha + \mathbf{i}''_\beta) \end{cases} \Rightarrow \begin{pmatrix} \mathbf{i}_A \\ \mathbf{i}_B \\ \mathbf{i}_C \end{pmatrix} = \frac{\sqrt{3}}{3a} \begin{pmatrix} 1 & 0 & -1 \\ -1 & 1 & 0 \\ 0 & -1 & 1 \end{pmatrix} \begin{pmatrix} \mathbf{i}''_\alpha \\ \mathbf{i}''_\beta \\ \mathbf{i}''_\gamma \end{pmatrix} \quad (7)$$

3. Power Management and MF-RPC Control Strategy

3.1. Power management

The power management strategy and control of MF-RPC have been designed by considering different working modes of the proposed system. It consists of two main sections. 1) PQ improving unit. 2) RBE utilization and ESSs control section.

3.1.1. PQ improving unit

The main duty of MF-RPC is dealing with PQ problems including imbalanced situation, harmonics, and reactive power. Assuming the PQ issues in case of saving energy in ESSs becomes more important. This part of MF-RPC can simultaneously suppress harmonics, balance voltages, and currents and improve power factor.

3.1.1. RBE utilization and ESSs control section

All possible modes for harvesting RBE in TSS include restoring to the grid, supplying adjacent trains and saving in ESSs. Depending on motoring/regenerating modes of locomotives in sections and RBE value, the proposed control method produces a suitable switching pattern for MF-RPC converters. The saved energy in ESSs (P_{ESS}) can be used for supplying substation loads. Declining the switching losses, the relation of power in MF-RPC can be calculated as (8).

$$P_{ESS} + P_\alpha + P_\beta = 0 \quad (8)$$

3.2. Current control method

The triple-loop modified control strategy is proposed to carry out all scenarios smartly. This method can manage the active powers (P_α, P_β) and reactive power (Q_α, Q_β) in α and β section together with charging and discharging active power in ESSs (P_{ESS}). The block diagram of the triple-loop control system is illustrated in Fig. 3. Using the SOGI-FLL and making π/2 lag in instantaneous voltages and currents [20], the obtained voltages and currents can be represented in αβ -coordinate system as (9)-(12).

$$\begin{pmatrix} V'_{\alpha\alpha}(t) \\ V'_{\beta\alpha}(t) \end{pmatrix} = \begin{pmatrix} \mathbf{Re}\left\{Ve^{i(\omega t+\psi)}\right\} \\ \mathbf{Re}\left\{Ve^{i(\omega t+\psi-\pi/2)}\right\} \end{pmatrix} \quad (9)$$

[DOI: 10.22068/IJRARE.7.2.35]

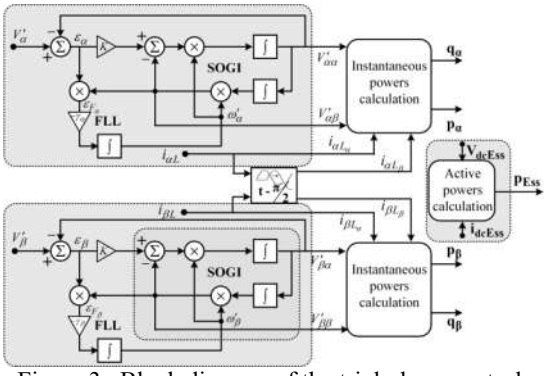

Figure 3. Block diagram of the triple-loop control system for proposed MF-RPC

$$\begin{pmatrix} V'_{\beta\alpha}(t) \\ V'_{\beta\beta}(t) \end{pmatrix} = \begin{pmatrix} \mathbf{Re}\left\{ V' e^{i(\omega t+\psi-\frac{\pi}{3})} \right\} \\ \mathbf{Re}\left\{ V' e^{i(\omega t+\psi-\frac{5\pi}{6})} \right\} \end{pmatrix} \quad (10)$$

$$\begin{pmatrix} i_{\alpha L_\alpha}(t) \\ i_{\alpha L_\beta}(t) \end{pmatrix} = \begin{pmatrix} \mathbf{Re}\left\{ I' e^{i(\omega t+\psi-\varphi_a)} \right\} \\ \mathbf{Re}\left\{ I' e^{i(\omega t+\psi-\frac{\pi}{2}-\varphi_a)} \right\} \end{pmatrix} \quad (11)$$

$$\begin{pmatrix} i_{\beta L_\alpha}(t) \\ i_{\beta L_\beta}(t) \end{pmatrix} = \begin{pmatrix} \mathbf{Re}\left\{ I' e^{i(\omega t+\psi-\frac{\pi}{3}-\varphi_b)} \right\} \\ \mathbf{Re}\left\{ I' e^{i(\omega t+\psi-\frac{5\pi}{6}-\varphi_b)} \right\} \end{pmatrix} \quad (12)$$

Where, V' and I' are the rms value of SrS voltage and currents. Based on IRP theory, the instantaneous active and reactive powers of α and β section can be calculated as follows:

$$\begin{pmatrix} \dot{p}_\alpha(t) \\ \dot{q}_\alpha(t) \end{pmatrix} = \begin{pmatrix} V_{\alpha\alpha}(t).i_{\alpha\alpha}(t) \\ V_{\beta\alpha}(t).i_{\alpha\alpha}(t) \end{pmatrix} + \begin{pmatrix} V_{\beta\alpha}(t).i_{\beta\alpha}(t) \\ -V_{\alpha\alpha}(t).i_{\beta\alpha}(t) \end{pmatrix} \quad (13)$$

$$\begin{pmatrix} \dot{p}_\beta(t) \\ \dot{q}_\beta(t) \end{pmatrix} = \begin{pmatrix} V_{\alpha\beta}(t).i_{\alpha\beta}(t) \\ V_{\beta\beta}(t).i_{\alpha\beta}(t) \end{pmatrix} + \begin{pmatrix} V_{\beta\beta}(t).i_{\beta\beta}(t) \\ -V_{\alpha\beta}(t).i_{\beta\beta}(t) \end{pmatrix} \quad (14)$$

The block diagram of the proposed IRP based control method with DC-Link voltage controller and modulation technique is shown in Fig. 4. Based on the fast dynamicity of ERS loads, numerical low pass filter (NLPF) are applied to separate DC parts of active powers which are responsible for NSC. To balance the currents, half of the power difference of the two sections and ESSs must be transferred from the heavily-loaded section to the lightly-loaded section. Meanwhile, to remove the inherent reactive power of the system caused by the secondary connection of TSS transformer, the common active power must be multiplied by a constant and added to the reactive powers [21]. The common powers of the two sections assuming ESSs are as follows:

$$\bar{p}_{com}(t) = \frac{\bar{p}_R(t) + \bar{p}_L(t) + \mathrm{P}_{Ess}}{2} \quad (15)$$

The required powers for generating the reference compensation currents can be calculated as:

The primary reference compensating currents can be calculated using the following equation.

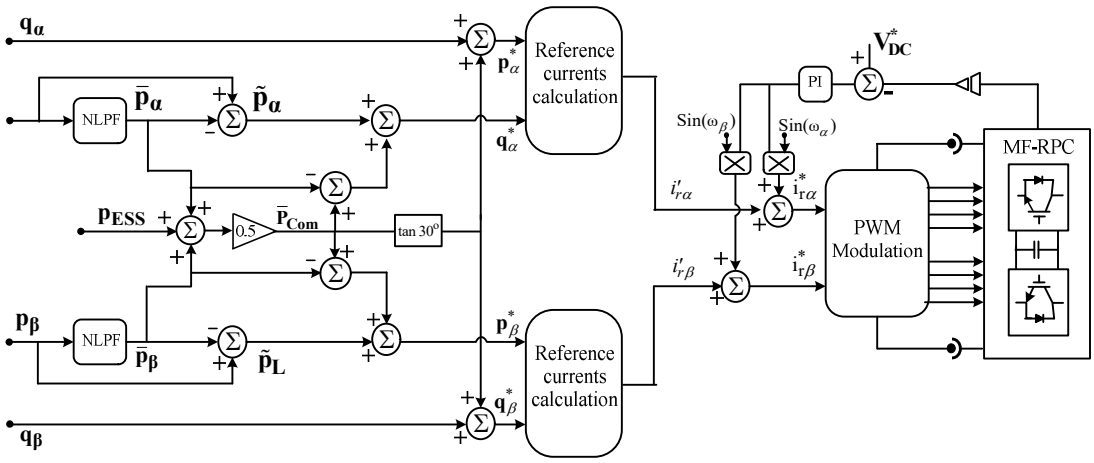

Figure 4. Block diagram of the proposed IRP based control method with DC-Link voltage controller and modulation technique

[DOI: 10.22068/IJRARE.7.2.35]

$$\begin{pmatrix} p_{\alpha}^{*}(t) \\ q_{\alpha}^{*}(t) \\ p_{\beta}^{*}(t) \\ q_{\beta}^{*}(t) \end{pmatrix} = \begin{pmatrix} \bar{p}_{com}(t) - \bar{p}_{\alpha}(t) + \tilde{p}_{\alpha}(t) \\ q_{\alpha}(t) + (\frac{1}{\sqrt{3}}\bar{p}_{com}(t)) \\ \bar{p}_{com}(t) - \bar{p}_{\beta}(t) + \tilde{p}_{\beta}(t) \\ q_{\beta}(t) - (\frac{1}{\sqrt{3}} \times \bar{p}_{com}(t)) \end{pmatrix} \quad (16)$$

3.3. The dc-link voltage control system

According to the proposed MF-RPC features and exchanging active power together with reactive power, the DC-link capacitor contains a high range of voltage fluctuation. To stabilize this voltage, a traditional PI controller is applied. This controller compares the reference voltage and DC-link voltage to generate the appropriate current control signals to make the voltage constant. The final reference currents can be extracted as:

$$\begin{cases} i'_{rR} = \dfrac{1}{V'^{2}_{\alpha\alpha}(t) + V'^{2}_{\beta\alpha}(t)} \begin{pmatrix} V_{\alpha\alpha}(t) & V_{\beta\alpha}(t) \end{pmatrix} \begin{pmatrix} p_{\alpha}^{*}(t) \\ q_{\alpha}^{*}(t) \end{pmatrix} \\ i'_{rL} = \dfrac{1}{V'^{2}_{\alpha\beta}(t) + V'^{2}_{\beta\beta}(t)} \begin{pmatrix} V_{\alpha\beta}(t) & V_{\beta\beta}(t) \end{pmatrix} \begin{pmatrix} p_{\beta}^{*}(t) \\ q_{\beta}^{*}(t) \end{pmatrix} \end{cases} \quad (17)$$

$$\begin{cases} i_{r\alpha}^{*} = i'_{r\alpha} + i_{\alpha loss} \\ i_{r\beta}^{*} = i'_{r\beta} + i_{\beta loss} \end{cases} \quad (18)$$

Where, $i_{\alpha loss}$ and $i_{\beta loss}$ are the loss currents related to the capacitor losses assigned by PI controller.

4. Simulation Results

To confirm the performance of proposed MF-RPC, simulations based on MATLAB software have been carried out. Due to the low

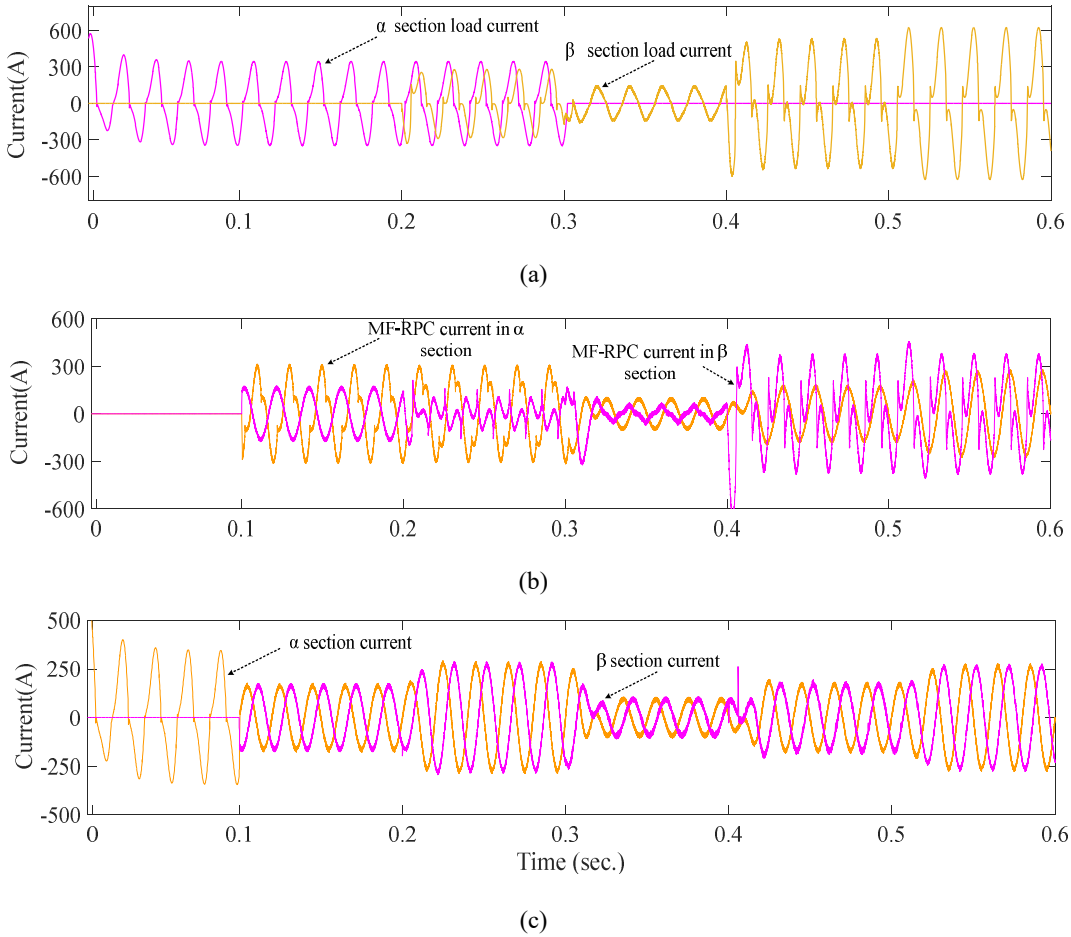

Figure 5. The measured current waveforms. a) consumed locomotive currents. b) MF-RPC currents. c) section currents

[DOI: 10.22068/IJRARE.7.2.35]

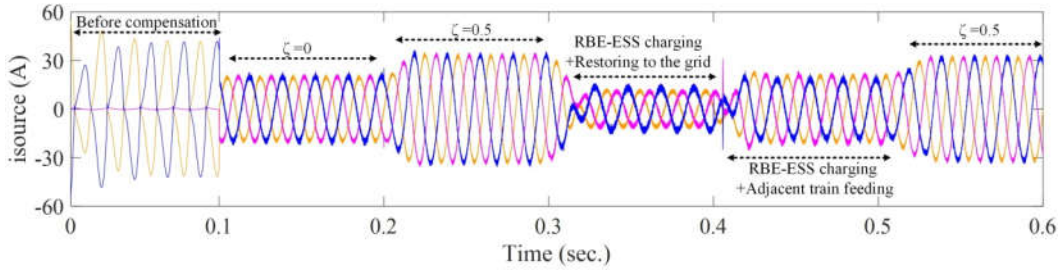

Figure 6. The three-phase grid-side currents for all six scenarios

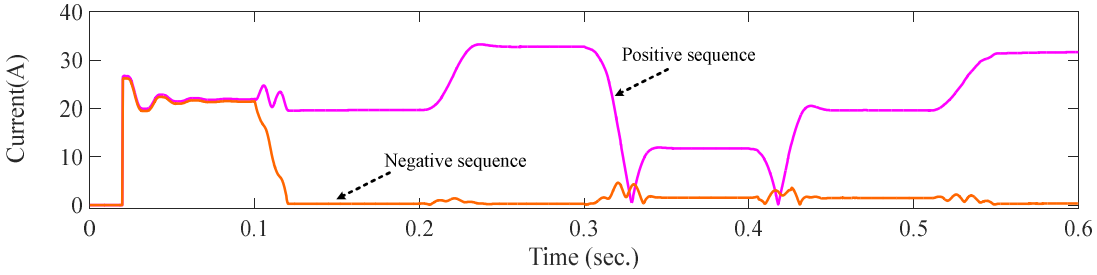

Figure 7. Positive and negative sequence current in grid-side

power factor and harmonic features of ERSs, locomotive loads are modeled as a full-controlled rectifier parallel with resistance and inductance. To have regenerative mode, a back EMF has been considered. To show all possible scenarios regarding the integration of ESS and RBE harvesting, the simulations are accomplished in six cases. In case 1, it is assumed one train in α section working in motoring mode and β section of the TSS has no train. Therefore, the load balanced ratio which is the power of the lightly-loaded section over the power of the heavily-loaded section is zero (ζ= 0). In case 2, the translocation of loads is the same as case 1 but, the proposed MF-RPC is switched on at t = 0.1 s. As shown in the currents waveforms of Fig. 5.a, the load currents ($i_{\alpha L}, i_{\beta L}$) are asymmetrical and full of harmonics. By injecting the compensation currents ($i_{\alpha t}, i_{\beta t}$) as Fig.5.b, the secondary side currents of sections (i_{α}, i_{β}) have been adjusted via interface inductances (L_I) and step-down transformers as demonstrated in Fig.5.c. The resulted network-side currents are depicted for all scenarios in Fig. 6. As shown in this figure, before MF-RPC operation the three-phase network-side currents are substantially imbalanced and asymmetrical.

The simulation results extracted in Table 1

Table 1. Simulation Results

	Operation conditions										
		Working modes of MF-RPC ports			Mode of RBE harvesting			THD;%			CIR%
	Interval	**Port** *α*	**Port** *β*	**Port** *ESS*	Saving to ESS	Supply adjacent train	Restore to the grid	*A*	*B*	*C*	
Case 1	0≤t<0.1	Motoring	No train	-	-	-	-	18.44	-	18.41	97.8
Case 2	0.1≤t<0.2	Motoring	No train	-	-	-	-	1.65	1.51	1.93	2.5
Case 3	0.2≤t<0.3	Motoring	Motoring	-	-	-	-	0.97	0.85	1.17	1.7
Case 4	0.3≤t<0.4	No train	Generating	P_{ESS}	✓	-	✓	2.87	3.62	3.81	7.1
Case 5	0.4≤t<0.5	Motoring	Generating	P_{ESS}	✓	✓	-	1.56	3.75	4.67	5.7
Case 6	0.5≤t<0.6	No train	Motoring	-	-	-	-	1.03	1.61	1.97	1.8

[DOI: 10.22068/IJRARE.7.2.35]

show that the current imbalanced ratio (CIR) which is almost 98% without compensation, has been decreased significantly to less than 7%. The positive and negative sequence currents shown in Fig. 7 confirm this performance. The related results for this figure show that the THD% of network-side three-phase currents which exceeds 18% in some cases has been mitigated significantly in all cases.

The case 3 denotes the mode that one train enters β section and both of the trains are in the motoring mode. Consequently, the absorbed active power from the utility grid is enhanced as shown in Fig. 8. Meanwhile, by operating of MF-RPC, the amount of absorbed reactive power is decreased near to zero. It reveals that the proposed MF-RPC can compensate for reactive power and improve the power factor of the system. In the next working mode, it is assumed that there is no train in α section and the train in β section is braking. In this case, since there is no consuming train in the section, most of the produced RBE is restored to the utility grid. As shown the Fig. 8, in this interval ($0.3 \leq t \leq 0.4$) the amount of active power is negative. Evaluating three-phase currents waveforms, the MF-RPC has sent the RBE to the grid sinusoidally and symmetrically. In addition, some of RBE is stored in the implemented battery-package based ESSs. The battery status waveforms are depicted in Fig. 9. These figures reveal that during interval $0.3 \leq t \leq 0.5$, the battery is actually recharged from the initial charging state of 10%. The negative amount of battery current shows the charging state of the battery pack. In case 5, the train in β section is in regenerative mode while a train in motoring mode enters α section. The motoring power is considered higher than the regenerated power. Consequently, some of the needed power for the motoring mode train is

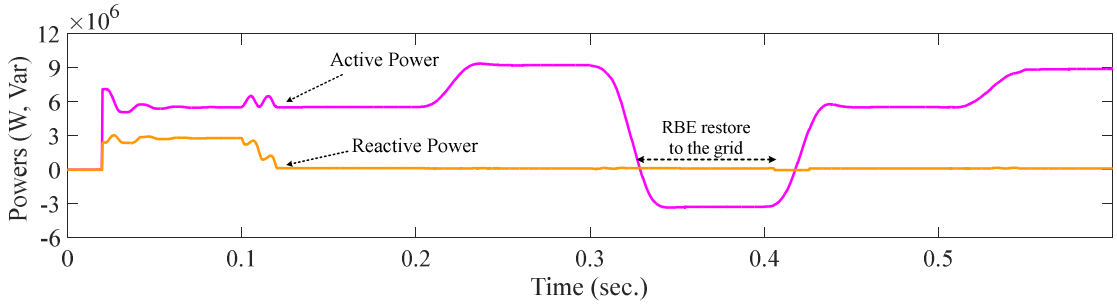

Figure 8. Active and reactive power in grid-side

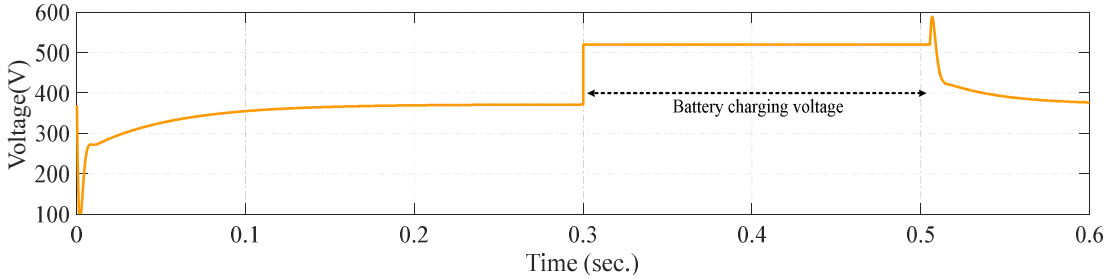

Figure 9. Battery package based ESS parameters: state of charge, current, and voltage

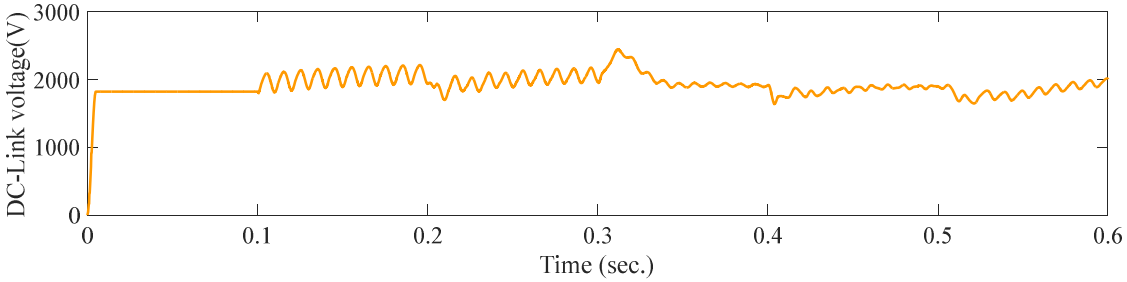

Figure 10. DC-link capacitor voltage waveform

[DOI: 10.22068/IJRARE.7.2.35]

supplied by produced RBE in the adjacent section and the rest provided by the utility grid

In the last scenario, the β section has a motoring mode train and α section is in no-load condition. Therefore, the charging of the battery pack is stoped. The stored energy in ESS can be used to supply TSS loads. To analyze the performance of PI controller for DC-link voltage of MF-RPC, The initial voltage of DC-link is assumed as 1700 V and the reference value is set to 2000V. The measured values of DC-link voltage during all scenarios are measured as Fig. 10. After applying MF-RPC, the control strategy regulates the capacitor voltage and makes it constant. It can be seen a little voltage fluctuation appears when the load power level is changed, but it is damped after regulation time. Hence, the control strategy is fast enough to respond to dynamic changes.

5. Conclusions

Harvesting of RBE in a.c. traction power supply system is rarely discussed in the past research. In this paper, an MF-RPC with triple-loop IRP based strategy is presented aiming to improve the energy consumption efficiency by RBE exploitation in ERS. The proposed MF-RPC operates as a smart energy hub with a high capability of optimal power exchange. It can restore the RBE to the utility grid based on the PQ standards, supply adjacent motoring mode trains and save generated energy in ESS located in TSS. To verify the performance of the proposed method, the precise simulations considering various load translocations and working modes have been carried out. The simulation results showed that, despite getting PQ improvement in PrS of TSS, the proposed MF-RPC system can be implemented as an interface multifunctional compensator to improve energy efficiency in ERSs and achieve benefits of ESSs.

References

[1] M. Brenna, F. Foiadelli, D. Zaninelli, “Electrical Railway Transportation Systems”, Hoboken, NJ, USA, Wiley-IEEE Press, 2018, pp. 263–296.

[2] S. V. Raygani, A. Tahavorgar, S. S. Fazel and B. Moaveni, "Load flow analysis and future development study for an AC electric railway," in *IET Electrical Systems in Transportation*, vol. 2, no. 3, pp. 139-147, September 2012.

[3] M. Brenna, F. Foiadelli, H. J. Kaleybar and S. S. Fazel, "Smart Electric Railway Substation Using Local Energy Hub Based Multi-Port Railway Power Flow Controller," *2019 IEEE Vehicle Power and Propulsion Conference (VPPC)*, Hanoi, Vietnam, 2019, pp. 1-6.

[4] Y. Song and W. Song, "A Novel Dual Speed-Curve Optimization Based Approach for Energy-Saving Operation of High-Speed Trains," *IEEE Trans. on Intell. Transp. Syst.*, vol. 17, no. 6, pp. 1564-1575, June 2016.

[5] F. Foiadelli, M. Roscia and D. Zaninelli, "Optimization of storage devices for regenerative braking energy in subway systems," *in Proc. IEEE Power Engin. Society General Meeting*, Montreal, Que., June 2006.

[6] İ. Şengör, H. C. Kılıçkıran, H. Akdemir, B. Kekezo&gcaron;lu, O. Erdinç and J. P. S. Catalão, "Energy Management of a Smart Railway Station Considering Regenerative Braking and Stochastic Behaviour of ESS and PV Generation," in *IEEE Trans. on Sustainable Energy*, vol. 9, no. 3, pp. 1041-1050, July 2018.

[7] Kaleybar, H.J., Kojabadi, H.M., Brenna, M., Foiadelli, F. and Zaninelli, D., 2017, June. “An intelligent strategy for regenerative braking energy harvesting in AC electrical railway substation” in *2017 5th IEEE International Conference on Models and Technologies for Intelligent Transportation Systems (MT-ITS)* (pp. 391-396).

[8] Y. Jiang et al."Energy Harvesting for the Electrification of Railway Stations: Getting a charge from the regenerative braking of trains.A," *IEEE Electrific. Mag.*, vol. 2, no. 3, pp. 39-48, Sept. 2014.

[9] Fazel, S.S., 2014. Energy-efficient emplacement of reversible DC traction power substations in urban rail transport through regenerative energy recovery. *International journal of railway research*, *1*(2), pp.11-22.

[10] M. Brenna, F. Foiadelli, E. Tironi and D. Zaninelli, "Ultracapacitors application for energy saving in subway transportation systems," *in Proc. IEEE Int. Conf. on Clean Elec. Power*, Capri, 2007, pp. 69-73.

[11] H. Moghbeli, H. Hajisadeghian and M. Asadi, "Design and simulation of hybrid electrical energy storage (HEES) for Esfahan

[DOI: 10.22068/IJRARE.7.2.35]

urban railway to store regenerative braking energy," *in Proc. IEEE 7th Power Elec. and Drive Syst.Tech. Con. (PEDSTC)*, Tehran, 2016, pp. 93-98.

[12] Z. Tian *et al*., "Energy evaluation of the power network of a DC railway system with regenerating trains," *IET Elec. Syst. in Transp.*, vol. 6, no. 2, pp. 41-49, 6 2016.

[13] P. Arboleya, B. Mohamed and I. El-Sayed, "DC Railway Simulation Including Controllable Power Electronic and Energy Storage Devices," in *IEEE Trans. on Power Systems*, vol. 33, no. 5, pp. 5319-5329, Sept. 2018.

[14] G. M. Scheepmaker and R. M. P. Goverde, "Energy-efficient train control including regenerative braking with catenary efficiency," *in Proc. IEEE Int. Con. on Intell. Rail Transport. (ICIRT)*, Birmingham, 2016, pp. 116-122.

[15] M. Shafighy, S. Khoo and A. Z. Kouzani, "Modelling and simulation of regeneration in AC traction propulsion system of electrified railway," *IET Elec. Syst. in Transp.*, vol. 5, no. 4, pp. 145-155, Dec. 2015.

[16] M. Ceraolo, G. Lutzemberger, A. Frilli and L. Pugi, "Regenerative braking in high speed railway applications: Analysis by different simulation tools," *in Proc. IEEE 16th Int. Con. on Envir. and Elec. Engin. (EEEIC)*, Florence, 2016, pp. 1-5.

[17] Y. Song and W. Song, "A Novel Dual Speed-Curve Optimization Based Approach for Energy-Saving Operation of High-Speed Trains," *IEEE Trans. on Intell. Transp. Syst.*, vol. 17, no. 6, pp. 1564-1575, June 2016.

[18] H. Hayashiya *et al*., "Regenerative energy utilization in a.c. traction power supply system," *in Proc. IEEE Inter. Power Elec. and Motion Cont. Conf. (PEMC)*, Varna, 2016, pp. 1125-1130.

[19] H. J. Kaleybar, S. Farshad, "A comprehensive control strategy of railway power quality compensator for AC traction power supply systems," *Turk. J. Elec. Eng. & Comp. Sci*, vol. 24, no. 6, 4582-4603, 2016.

[20] Kaleybar, H.J., Kojabadi, H.M., Foiadelli, F., Brenna, M. and Blaabjerg, F., 2019. Model analysis and real-time implementation of model predictive control for railway power flow controller. *International Journal of Electrical Power & Energy Systems*, *109*, pp.290-306.

[21] Kaleybar, H.J., Kojabadi, H.M., Fazel, S.S. and Foiadelli, F., 2018. An intelligent control method for capacity reduction of power flow controller in electrical railway grids. *Electric Power Systems Research*, *165*, pp.157-166.

[DOI: 10.22068/IJRARE.7.2.35]